PERGAMON

International Journal of Heat and Mass Transfer 44 (2001) 2957–2964

International Journal of HEAT and MASS TRANSFER

www.elsevier.com/locate/ijhmt

Bubble nucleation in microchannels: statistical mechanics approach

X.F. Peng [a,*], Y. Tien [a], D.J. Lee [b]

[a] *Department of Thermal Engineering, Tsinghua University, Beijing 100084, People's Republic of China*
[b] *Department of Chemical Engineering, Taiwan University, Taipei 106, People's Republic of China*

Received 6 December 1999; received in revised form 17 September 2000

Abstract

Microscale boiling displays quite some unusual characteristics, like the occurrence of the so-called "fictitious boiling". This paper modeled the bubble embryos occurring during microchannel boiling using a statistical mechanics approach. The bubble nucleation temperature of working liquid heated in a microchannel was theoretically derived. Experimental efforts were conducted to measure the nucleation temperatures for four working fluids (water, methanol, ethanol and carbon tetrachloride) boiled on a platinum wire confined in capillary tubes. Both theoretical and experimental findings demonstrated that the bubble nucleation temperature markedly increased as the size of microchannel went down. Regression analysis of experimental results estimated the process parameters in the theoretical prediction.

Keywords: Microchannel boiling; Bubble embryo; Statistical mechanics; Phase transition

1. Introduction

Microchannel boiling has attracted research efforts worldwide for its potential application in electronic cooling [1]. The formation of vapor bubbles in microchannel boiling is not favorable, since they could block out the microchannel and break down the heating apparatus. Nevertheless, researchers noted that it is extremely difficult to generate bubbles even at a very high heat flux from heater allocated in microchannels [2,3]. Peng and co-workers [4–9] conducted a series of experimental investigations on the flow boiling in microchannels. They also noted the so-called "bubble-extinction" behavior of microchannel boiling. That is, at a high heat flux that is sufficient to induce vigorous nucleate boiling mode on a normal-sized heater or in normal-sized channels, one could hardly observe vapor bubble on a microchannel heater. Such an observation made a distinction between microchannel boiling and the normal boiling.

To interpret the bubble-extinction behavior observed in microchannel boiling, Peng and Wang [10] proposed the concepts of "evaporating space" and "fictitious boiling". The former concept stated that there exists a critical liquid space less than which normal bubbles could not successfully form and grow. For the latter, in microchannel small bubble embryos could actually form, however, since their size could not grow up to exceed the critical radius of bubble (r_C) formulated by conventional nucleation theory [11], eventually collapse. A physical picture for fictitious boiling was suggested for fictitious boiling as to have crowded tiny bubbles (bubble embryos) grow and collapse rapidly and continuously, thereby mimicking a boiling state and transferring a large amount of heat. Some mechanistic interpretations are required to add on Peng and Wang's proposition as to why only in microchannel the growth of bubble embryos could be depressed.

Peng et al. [12] and Liu [13] provided a thermodynamic analysis to the inactivation of bubble growth using either classical theory [14,15] or molecular theory [16–18]. With the assumption that some excess pressure

* Corresponding author. Tel.: +86-10-6278-9751; fax: +86-10-6277-0209.
E-mail address: pxf-dte@mail.tsinghua.edu.cn (X.F. Peng).

0017-9310/01/$ - see front matter
PII: S0017-9310(00)00323-9

Nomenclature

c_1, c_2	proportionality constant
D	diameter of capillary tube
d	diameter of heating wire
d_e	diameter of bubble embryos
E_{ave}	average energy of the embryo
F	free energy of the embryo
F_{max}	maximum free energy of the embryo
H	Hamiltonian of the cluster
h	Planck constant
k	Boltzmann constant
L	length of heating wire
m	mass of fluid molecule
N	number of molecules in the cluster
N_l	number of molecules in sub-system l
r_C	critical radius of bubble or active nucleation site
T	temperature
T_{max}	bubble nucleation temperature
U	propagation velocity of pressure wave
V	volume of the cluster
V_l	volume of the sub-system l
V_{max}	threshold system volume where $T_{max} = T_{max,max}$
Z	partition function for the ensemble

Greek symbols

Γ	function defined in Eq. (11b)
Λ	function defined in Eq. (11a)
ρ_N	number density ($=N/V$)
ε	total energy of embryo
ε_l	energy for sub-system$_l$
$\varepsilon_{l,max}$	maximum energy level for embryo
$\varepsilon_{l,min}$	minimum energy level for embryo
Ω	state density
Ψ_l	state vector for sub-system l
σ	standard deviation of distribution

would be exerted onto the bubble embryos owing to the existence of confined walls, Peng et al. [19] correlated the superheat data for bubble nucleation with the microchannel size. However, these authors have no idea of what had caused the local pressure increase around bubble embryos.

In a subsequent work, Peng et al. [20] conducted a population balance analysis on bubble embryos existing in a superheated liquid. These authors, with the assistance of some constitutive equations relating the growth and collapse rates of the embryos, demonstrated that the presence of certain external perturbations could largely depress the size of embryos, whence yielding fictitious boiling of liquids. The source of external perturbations was proposed to be the impulse pressure wave generated accompanied with the emergence of embryos, which could be reflected back by the confined wall to smash off the embryo.

To explore this point further, Peng et al. [21] estimated the propagation velocity of impulse pressure wave for a van der Waals liquid and, using the growth time of embryo and channel size as parameters, proposed a geometric criterion for the occurrence of fictitious boiling. For example, for water at 120°C and 0.1 MPa, these authors proposed that normal nucleate boiling could not be sustained if the channel size is less than approximately 2.4 mm, which correlates with the experimental evidences.

As discussed above, good advances were achieved toward the in-depth understanding on microchannel boiling. However, most literature models are based on various kinds of continuous mechanics approximations. Bubble embryos in a superheated liquid are small clusters of high-energy fluid molecules. Quantum effects could be predominant for the dynamic characteristics of these clusters. This paper conducted an analysis on the bubble nucleation from a superheated liquid confined in microchannel. Experimental efforts were devoted for four working fluids to demonstrate the size effects from which the process parameters were estimated.

2. Nucleation temperature in microchannel

We considered herein the bubble embryo (the cluster) under investigation as a canonical ensemble which comprises a fixed amount of fluid molecules (N) and fixed fluid volume (V), and can exchange energy with a heat batch at a constant temperature of (T). The heat bath is so large that the bath energy is much larger than the energy of the embryo. Therefore, the energy levels of the bath could be regarded as continuous. A diathermal, rigid and impermeable boundary is assumed for dividing the embryo and the heat bath.

Only the potential clusters that might become a real vapor bubble are of interest herein. Therefore, only the ones that comprise a large amount of molecules with size close to r_C are further interpreted.

Schematically, we can imagine the embryo to be comprised of many sub-systems that are of N_l fluid molecules, volume V_l, and energy ε_l's, which are the eigenvalues of the Schrodinger's equation $H\Psi_l = \varepsilon_l\Psi_l$, where H is the Hamiltonian operating on the state vector Ψ_l. Thus, we have the following identities for the embryo:

$$N = \sum_l N_l, \tag{1}$$

$$V = \sum_l V_l, \tag{2}$$

$$\varepsilon = \sum_l \varepsilon_l. \tag{3}$$

Thermal equilibrium is achieved between the embryo and the heat bath. The number of states for the embryo with N, V and energy between ε_l and $\varepsilon_l + \mathrm{d}\varepsilon_l$ could be stated as follows:

$$\Omega(\varepsilon)\mathrm{d}\varepsilon = 2\pi V\left(\frac{2m}{h^2}\right)^{3/2}\varepsilon_l^{1/2}\mathrm{d}\varepsilon_l, \tag{4}$$

where m and h are the mass of fluid molecule and the Planck constant, respectively. Normally the growth (and collapse as well) of bubble embryo is so fast that the total system, the embryo and the heat bath, could be regarded as isolated. Hence the free energy of the system could be expressed as follows

$$F = -NkT\ln Z, \tag{5}$$

where k is the Boltzmann constant, and Z is the canonical partition function defined as

$$Z = \sum_l 2\pi V\left(\frac{2m}{h^2}\right)^{3/2}\varepsilon_l^{1/2}\exp\left(-\frac{\varepsilon_l}{kT}\right)\mathrm{d}\varepsilon_l. \tag{6}$$

Many energy levels exist for microparticles in the embryo, the summation in Eq. (6) could be approximated by an integral. Hence, the free energy per unit volume of fluid could be stated as follows:

$$F_V = \frac{F}{V} = -\rho_N kT\ln\left\{\int_0^\infty 2\pi V\left(\frac{2m}{h^2}\right)^{3/2}\varepsilon^{1/2}\times\exp\left(-\frac{\varepsilon_l}{kT}\right)\mathrm{d}\varepsilon\right\}. \tag{7}$$

where ρ_N is the particle density ($=N/V$).

The particles having energy levels at both the extremes of integral are rare, while most of them could be allocated between the range $[\varepsilon_{l,\max}, \varepsilon_{l,\min}]$. According to mean-value theorem, there exists an energy level E_{ave} that belongs to this range which makes the following approximation to be held:

$$F_V \approx -\rho_N kT\ln\left\{2\pi V\left(\frac{2m}{h^2}\right)^{3/2}E_{\mathrm{ave}}^{1/2}\exp\left(-\frac{E_{\mathrm{ave}}}{kT}\right)\times(\varepsilon_{l,\max}-\varepsilon_{l,\min})\right\}. \tag{8}$$

At $T = T_{\max}$ where phase transition occurs, $F_V = F_{V,\max}$. Restated, the system temperature could be rearranged as follows:

$$T_{\max} \approx \frac{E_{\mathrm{ave}} - (F_{V,\max}/\rho_N)}{k\ln\left\{2\pi V(2m/h^2)^{3/2}E_{\mathrm{ave}}^{1/2}(\varepsilon_{l,\max}-\varepsilon_{l,\min})\right\}}. \tag{9}$$

The energy levels of all sub-systems or particles in the embryo change with temperature. Hence, the parameters F_V, E_{ave}, $\varepsilon_{l,\max}$, and $\varepsilon_{l,\min}$ increase with temperature T. Notably, the energy distribution is Gaussian-like if the numbers of fluid molecules and energy states in the embryo are both large. Hence, $(\varepsilon_{l,\max} - \varepsilon_{l,\min}) = c\sigma$, where σ is the standard deviation of the distribution and $\sigma^2 = kT^2(\partial E_{\mathrm{ave}}/\partial T)_V$. c is a proportional constant. Therefore, the denominator of Eq. (9) is proportional to $\ln\{T^2 E_{\mathrm{ave}}(\partial E_{\mathrm{ave}}/\partial T)_V\}$, which changes slower than its numerator.

The size effects are of main concern in this work. We can speculate that the embryo size would be larger if the confined microchannel increases in its scale (discussed later). Both the numerator and denominator of Eq. (9) will have to have the same sign for a physically relevant system. This is the case since at large V, $E_{\mathrm{ave}} \gg F_{V,\max}/\rho_V$ and the value in the logarithm of the denominator of Eq. (9) exceeds unity. On the contrary, at the $V \to 0$ limit, $E_{\mathrm{ave}} \ll F_{V,\max}/\rho_V$ and the logarithm in the denominator changes sign as well.

Similar qualitative discussions could be employed for demonstrating the dependence of liquid superheat ($T_{\max} - T_{\mathrm{sat}}$) required for bubble nucleation as a function of system volume, V. Fig. 1 schematically depicts such a dependence. As the system volume decreases from a normal sized channel ($V \to \infty$), the required superheat increases accordingly, since in this case $E_{\mathrm{ave}} \gg F_{V,\max}/\rho_V$, $T_{\max}$ inversely depends on $\ln(V)$. At another

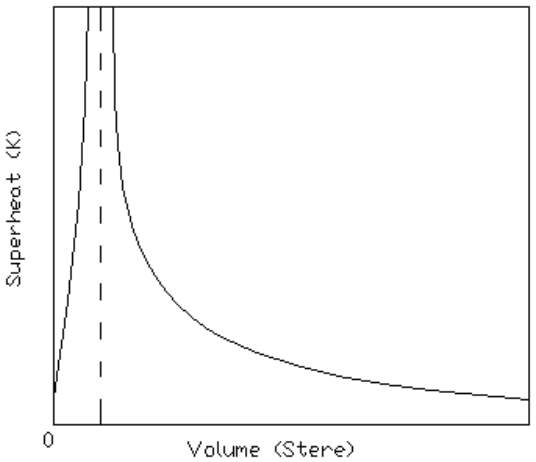

Fig. 1. Effect of scale on boiling nucleation superheat.

extreme where $V \to 0$, $E_{ave} \gg F_{V,max}/\rho_V$, therefore both the numerator and denominator of Eq. (9) depend on $\ln(V)$ and cancel out each other. (It is also noteworthy that $F_{V,max}/\rho_V$ grows with $\ln(V)$.) T_{max} hence approaches a constant. For the case of extremely small confined space or comparable to particle size, the temperature decreases with the decrease of the volume, as shown in Fig. 1. This case actually means the phase change seems no significance. Apparently there exists a threshold system volume V_{max} where T_{max} reaches a peak value ($T_{max,max}$). Nevertheless, $T_{max,max}$ should not exceed the superheat limit for the specific working liquid. The dependence of T_{max} on system volume is distinct relying on the range of the system volume. For normal fluids V_{max} is generally much smaller than the most practical situations. Hence, one would observe increased liquid superheat needed to trigger bubble nucleation when the size of microchannel heater went down.

3. Experimental

Fig. 2 schematically depicts the experimental setup. A capillary tube filled with saturated working fluid was the heating vessel, along the centerline a platinum (Pt) wire of diameter 0.03 mm (d) and of length 25 mm (L) was hanged between two electrodes. A DC current was applied for heating. With the assistance of wire's electrical resistance versus temperature correlation, the surface temperature of the Pt wire could be calculated from the electric current and voltage drop data. The liquid temperature was measured by thermocouples in two outside liquid reservoirs. Other experimental details were described by Tien [22]. Bubble embryos would form in the superheated liquid layer adjacent to the heating surface. Restated, the surface temperature of Pt wire is taken as the system temperature of embryo. Three capillary tubes were employed in this work, which were of 1, 0.5, and 0.3 mm in diameter (D), respectively. Four working fluids were herein tested: water, methanol (CH_3OH), ethanol (C_2H_5OH) and carbon tetrachloride (CCl_4).

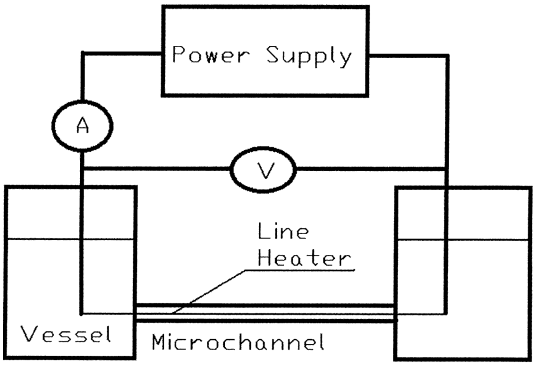

Fig. 2. Experimental setup.

In each test, the capillary tube was first filled with saturated, degassed working fluid. Then the DC current through the Pt wire was increased very slowly. The electric voltage drop and the current data were continuously recorded till bubble nucleation occurred. High-resolution CCD camera recorded the boiling dynamics.

4. Results and discussion

4.1. Superheat to bubble nucleation

Table 1 lists the experimental results for the superheat required to bubble nucleation (T_{max}). As expected, although with certain data scattering, T_{max} markedly increases with decreasing capillary tube diameter. Take CCl_4 as an example. The corresponding $T_{max} = 5.3$ K when $D = 1$ mm; while $T_{max} = 69$ K at $D = 0.3$ mm. Such an observation correlates with the literature results. On the other hand, the water test at 1.0 mm capillary tube reveals early boiling at 95°C, or a negative superheat of −5 K. Such an discrepancy has not been noted in the other three organic working fluids.

Figs. 3–6 compare the experimental results with the semi-empirical correlation proposed by Peng et al. [8]. Greater data scattering is noted for water tests. Such an observation might be attributed to residual dissolved gas in the water bath. On the other hand, satisfactory agreement is achievable for the other three organic working fluids. In general, Peng et al.'s correlation could describe the superheats for bubble nucleation in microchannel boiling.

Table 1
Superheat required for bubble nucleation

Capillary tube (mm)	$T_{max} - T_{sat}$ (K)			
	Water	Methanol	Ethanol	CCl_4
1.00	−5.0	9.7	10.0	5.3
0.50	23.1	35.2	19.7	21.0
0.30	67.3	55.7	51.1	69.2

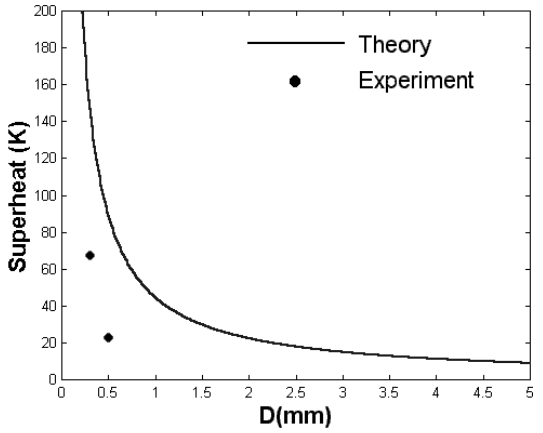

Fig. 3. Comparison of measurements with the prediction for water.

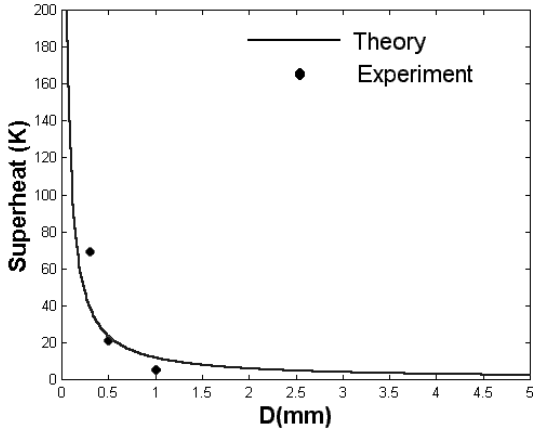

Fig. 4. Comparison of measurements with the prediction for carbon tetrachloride.

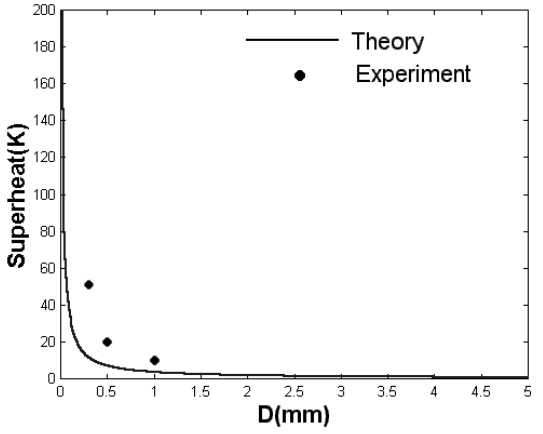

Fig. 5. Comparison of measurements with the prediction for methanol.

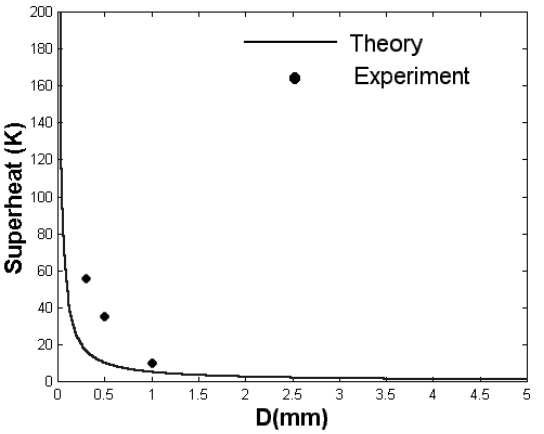

Fig. 6. Comparison of measurements with the prediction for ethanol.

4.2. Microphotographic observations

Figs. 7–10 represent some microphotographic observations of the boiling tests in 0.30 mm capillary tube.

Fig. 7 demonstrates the junction section between the capillary tube and the outside reservoir, in which CCl_4 is subject to a superheat of 11 K. No bubbles are formed inside the capillary tube. However, large bubbles appear at the junction port. Restated, the superheated liquid cannot transform into vapor phase within the 0.3 mm capillary tube. However, once the superheated liquid is released to the un-confined space, normal bubble nucleation occurs.

Fig. 8 illustrates the phenomenon noted for CCl_4 boiled at superheat of 69 K on the Pt wire. Many small bubbles apparently appear around the wire in the capillary tube and they vigorously oscillate along the axial direction of tube.

In Figs. 9 and 10, the boiling processes for methanol and for ethanol with wire temperature close to their corresponding T_{max} are shown. No visible bubbles could be detected. However, the liquid oscillates so vigorously that the heating Pt wire has been masked and has been invisible.

Therefore, a physical picture could be summarized from the experimental observations of the four working fluids tested herein. In a microchannel, the liquid temperature could be increased up to much exceeding the heterogeneous nucleation temperature of bubbles without detectable bubble formation or liquid motion. However, when the liquid temperature approaches T_{max}, chaotic vibrations of superheated liquid become visible. Such an observation might be attributed to the vigorous growth/collapse of bubble embryos in the superheated liquid. At T_{max}, vapor bubbles emerge from the whole body of the superheated liquid layer. If the microchannel is small enough and the cross flow liquid velocity is not

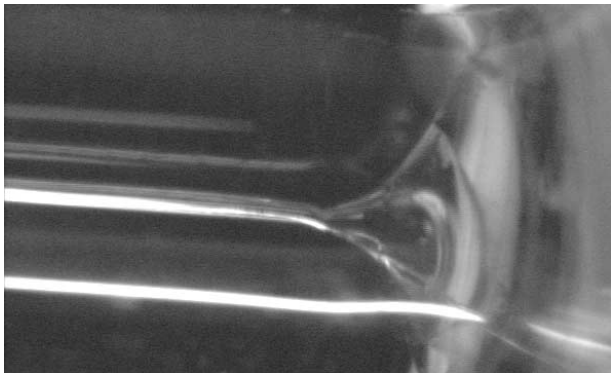

Fig. 7. Boiling nucleation observation for water.

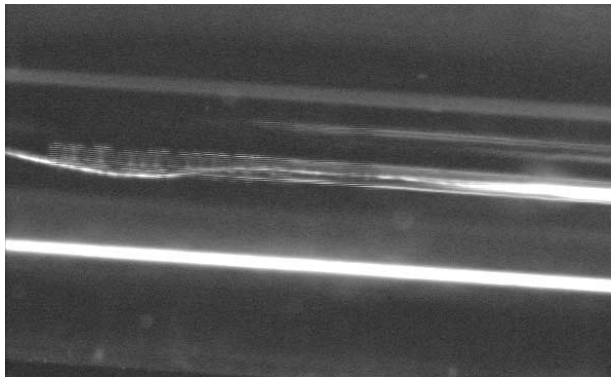

Fig. 8. Boiling nucleation observation for carbon tetrachloride.

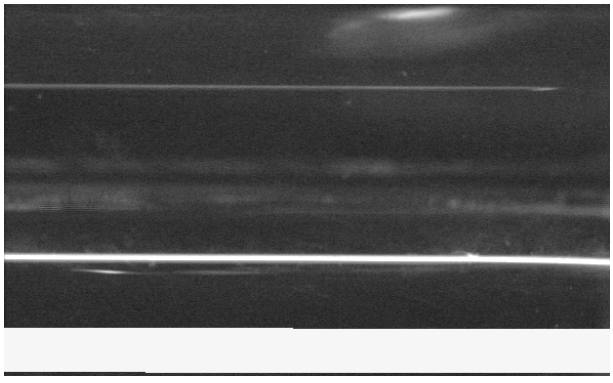

Fig. 9. Boiling nucleation observation for methanol.

strong enough to sweep out these vapors, the heating device simply dries out.

4.3. Data interpretation

Eq. (9) describes the data of T_{max} as a function of complicated process parameters and embryo volume V. Although one speculates that the volume of bubble embryo increases with the void space in the capillary tube, it would not be feasible for any subsequent analysis if the embryo volume could not be satisfactorily estimated.

Peng et al. [11] estimated the propagation velocity of impulse pressure wave (U) in the liquid for a van der

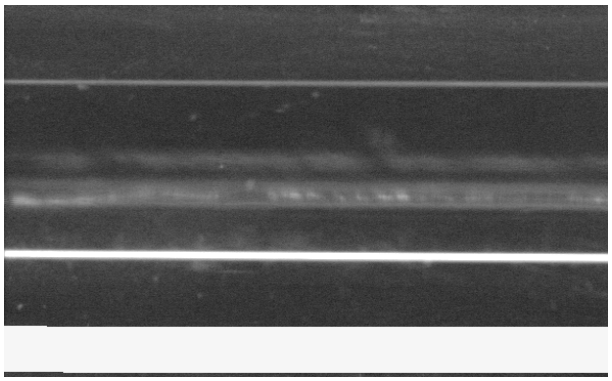

Fig. 10. Boiling nucleation observation for ethanol.

Waals liquid. These authors claimed that the emergence of a bubble embryo would generate an impulse pressure wave that spreads outward. Part of this impulse pressure wave could be reflected from the capillary wall hence depress the embryo growth if it has not grown up to r_C at the wave's arrival. Hence, the size of the embryo can grow depends on the elapsed time the pressure wave needs to travel. Most of bubble embryos would be generated close to the heating wire surface. Therefore, the traveling distance of pressure wave is $(D-d)/2$, which is proportional to the embryo growth time. For small embryos their growth rate could be taken as proportional to the growth time. Hence, the embryo could have a diameter of d_e that is proportional to $(D-d)$. Therefore, the volume of embryo could be taken as proportional to $(D-d)^2$ or $V = c_2(D-d)^3$.

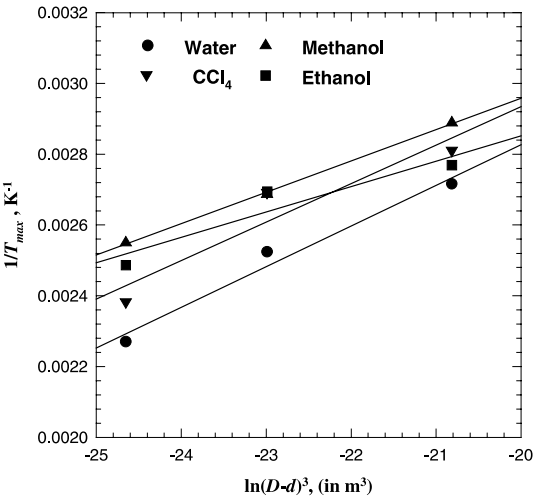

Fig. 11. Correlation of the superheat and geometrical scale.

Over a limited temperature range, the change in the numerator (hence the denominator as well) of Eq. (9) could be ignored and Eq. (9) could therefore be approximated by the following linear form:

$$\frac{1}{T_{\max}} = \frac{\ln \Lambda}{\Gamma} + \frac{1}{\Gamma}\ln(D-d)^3, \tag{10}$$

where

$$\Lambda = 2\pi c_2 \left(\frac{2m}{h^2}\right)^{3/2} E_{\text{ave}}^{1/2}(\varepsilon_{l,\max} - \varepsilon_{l,\min}), \tag{11a}$$

$$\Gamma = \frac{1}{k}\left(E_{\text{ave}} - \frac{F_{V,\max}}{\rho_N}\right). \tag{11b}$$

In Eq. (10) we proposed a regression scheme for estimating the parameters Λ and Γ using linear regression analysis. Fig. 11 illustrates the $1/T_{\max}$ versus $\ln(D-d)^3$ plot. Notably all curves could be approximated by a linear function, hence, the assumption that the changes in the numerator and the denominator of Eq. (9) could be safely ignored.

Table 2 lists the best-fitted parameters Λ and Γ using linear regression analysis. Notably, the regression coefficient all exceed 0.89, with some of them being greater

Table 2
Estimated parameters in Eq. (9) using linear regression analysis

	Water	Methanol	Ethanol	CCl_4
Λ (m^{-3})	2.42×10^{19}	1.51×10^{23}	9.50×10^{25}	2.57×10^{20}
$k\Gamma$ (J)	1.20×10^{-19}	1.56×10^{-19}	1.89×10^{-19}	1.27×10^{-19}
Regression coefficient	0.976	0.999	0.889	0.902

than 0.99. These parameters could be used in engineering applications for predicting the bubble nucleation temperature. Notably, $1/\Lambda$ reflects a characteristic volume of the system, while $k\Gamma$ denotes the energy barrier for bubble nucleation.

The superheat limit for liquid water is 543 K. No liquid could exist at atmospheric pressure if its temperature exceeds this limit. Substituting $T_{max} = 543$ K into Eq. (9) yields the critical gap between D and d ($D - d$) could be estimated as 73 μm. Restated, if the diameter of the capillary tube is set less than 0.073 mm, the water could sustain its liquid state up to the superheat limit.

5. Conclusions

To generate vapor bubbles during microchannel boiling is much more difficult than normal situations. Peng and co-workers proposed that bubble embryos continuously emerged and collapsed in the superheated liquid that transferred a large amount of heat without the formation of large, stable vapor bubbles. This paper analyzed the so-called "fictitious boiling" process by modeling the bubble embryos as clusters comprised of high-energy molecules. Theoretical correlation between bubble nucleation temperature was derived showing the effects of microchannel size. Experimental efforts were conducted to measure the nucleation temperatures for four working fluids (water, methanol, ethanol, and carbon tetrachloride) boiled on a platinum wire confined in capillary tubes. Both theoretical and experimental findings demonstrated that the bubble nucleation temperature markedly increased as the size of microchannel went down. Microphotographic observations suggested that close to bubble nucleation temperature the liquid would vigorously oscillate in the microchannel, which might be attributed to the emergence of tiny bubble embryos. Based on regression analysis of experimental results the process parameters in the theoretical prediction were estimated.

Acknowledgements

This research is currently supported by the National Natural Science Foundation of China through contract No. 59625612 and 59976016.

References

[1] M.B. Bowers, I. Mudawar, High flux boiling in low flow rate, low pressure drop mini-channel and microchannel heat sinks, Int. J. Heat Mass Transfer 37 (1994) 321–332.

[2] L. Lin, A.P. Pisano, Bubble forming on a micro line heater, micromechanical sensors, actuators, and systems, ASME DSC 32 (1991) 147–164.

[3] L. Lin, K.S. Udell, A.P. Pisano, Liquid–vapor phase transition and bubble formation in micro structures, Therm. Sci. Eng. 2 (1994) 52–59.

[4] X.F. Peng, B.X. Wang, Forced-flow convection and flow boiling heat transfer for liquid flowing through microchannels, Int. J. Heat Mass Transfer 36 (1993) 3421–3427.

[5] X.F. Peng, B.X. Wang, Liquid flow and heat transfer in microchannels with/without phase change, in: Proceedings of the 10th International Heat Transfer 1, 1994, p. 159–177.

[6] X.F. Peng, G.P. Peterson, Flow boiling of binary mixtures in microchanneled plates, Int. J. Heat Mass Transfer 39 (1996) 1257–1264.

[7] X.F. Peng, B.X. Wang, Forced-convection and boiling characteristics in microchannels, in: Proceedings of the 11th International Heat Transfer 1, 1998, p. 371–390.

[8] X.F. Peng, H.Y. Hu, B.X. Wang, Boiling nucleation during liquid flowing in microchannels, Int. J. Heat Mass Transfer 41 (1998) 101–106.

[9] H.Y. Hu, G.P. Peterson, X.F. Peng, B.X. Wang, Interface fluctuation propagation and superposition model for boiling nucleation, Int. J. Heat Mass Transfer 41 (1998) 3483–3490.

[10] X.F. Peng, B.X. Wang, Evaporation space and fictitious boiling for internal evaporation of liquid, Science Foundation in China 2 (1994) 55–59.

[11] V.P. Carey, Liquid–Vapor Phase Change Phenomena, Taylor and Francis, New York, 1992.

[12] X.F. Peng, H.Y. Hu, B.X. Wang, Boiling formation of liquid boiling in microchannels, Sci. China, Ser. E 41 (1998) 404–410.

[13] D. Liu, Heat transfer and boiling nucleation of liquid in microscale structures, Master thesis, Tsinghua University, Beijing, China, 1999.

[14] V.P. Skripov, Metastable Liquids, Wiley, NY, 1974 (Chapter 2).

[15] J.W. Westwater, Boiling of liquids, Adv. Chem. Eng. 2 (1958) 1–56.

[16] H.Y. Kwak, S. Lee, Homogeneous bubble nucleation predicted by a molecular interaction model, ASME J. Heat Transfer 113 (1991) 714–721.

[17] H.Y. Kwak, Y.W. Kim, Homogeneous nucleation and macroscopic growth of gas bubble in organic solutions, Int. J. Heat Mass Transfer 41 (1998) 757–767.

[18] S. Kotake, Molecular clusters, in: C.L. Tien (Ed.), Microscale Energy Transport, 1998 (Chapter 5).

[19] X.F. Peng, H.Y. Hu, B.X. Wang, Flow boiling through V-shape microchannels, Exp. Heat Transfer 11 (1998) 87–100.

[20] X.F. Peng, D. Liu, D.J. Lee, Y. Yan, Cluster dynamics and fictitious boiling in microchannels, Int. J. Heat Mass Transfer 43 (2000) 4259–4265.

[21] X.F. Peng, D. Liu, D.J. Lee, Y. Yan, Dynamic characteristics of microscale boiling, Heat Mass Transfer, 2000, in press.

[22] Y. Tien, Theoretical and experimental investigation of the influence of spatial scale on nucleate boiling, Unpublished Report, Tsinghua University, Beijing, 2000.